Journal of Clinical Monitoring and Computing (2022) 36:775–783
https://doi.org/10.1007/s10877-021-00708-x

ORIGINAL RESEARCH

Accuracy of noncontact surface imaging for tidal volume and respiratory rate measurements in the ICU

Erwan L'Her[1,2] · Souha Nazir[2] · Victoire Pateau[1] · Dimitris Visvikis[2]

Received: 11 December 2020 / Accepted: 13 April 2021 / Published online: 22 April 2021

Abstract

Tidal volume monitoring may help minimize lung injury during respiratory assistance. Surface imaging using time-of-flight camera is a new, non-invasive, non-contact, radiation-free, and easy-to-use technique that enables tidal volume and respiratory rate measurements. The objectives of the study were to determine the accuracy of Time-of-Flight volume (VT_{TOF}) and respiratory rate (RR_{TOF}) measurements at the bedside, and to validate its application for spontaneously breathing patients under high flow nasal canula. Data analysis was performed within the ReaSTOC data-warehousing project (ClinicalTrials.gov identifier NCT02893462). All data were recorded using standard monitoring devices, and the computerized medical file. Time-of-flight technique used a Kinect V2 (Microsoft, Redmond, WA, USA) to acquire the distance information, based on measuring the phase delay between the emitted light-wave and received backscattered signals. 44 patients (32 under mechanical ventilation; 12 under high-flow nasal canula) were recorded. High correlation ($r = 0.84$; $p < 0.001$), with low bias (-1.7 mL) and acceptable deviation (75 mL) was observed between VT_{TOF} and VT_{REF} under ventilation. Similar performance was observed for respiratory rate ($r = 0.91$; $p < 0.001$; bias < 1b/min; deviation ≤ 5b/min). Measurements were possible for all patients under high-flow nasal canula, detecting overdistension in 4 patients (tidal volume > 8 mL/kg) and low ventilation in 6 patients (tidal volume < 6 mL/kg). Tidal volume monitoring using time-of-flight camera (VT_{TOF}) is correlated to reference values. Time-of-flight camera enables continuous and non-contact respiratory monitoring under high-flow nasal canula, and enables to detect tidal volume and respiratory rate changes, while modifying flow. It enables respiratory monitoring for spontaneously patients, especially while using high-flow nasal oxygenation.

Keywords Respiratory monitoring · Tidal volume · VILI · P-SILI · Time-of-flight

Abbreviations

ICU	Intensive Care Unit
VT	Tidal volume
VT_{TOF}	Tidal volume measured using the Time-of-Flight camera
VT_{REF}	Tidal volume measured by the mechanical ventilator
RR	Respiratory rate
RR_{TOF}	Respiratory rate measured using the Time-of-Flight camera
VILI	Volume-induced lung injury
P-SILI	Patient self-inflicted lung injury
HFNC	High-flow nasal cannula
EIT	Electrical impedance tomography
TOF	Time-of-Flight imaging
RGB	Red, green, and blue camera
IR	Infrared
ROI	Region of interest
SD	Standard deviation
MV	Mechanical ventilation
CW	Continuous wave
SLP	Structured light plethysmography
OEP	Optoelectronic plethysmography
PEEP	Positive end expiratory pressure
ARDS	Acute respiratory distress syndrome

✉ Erwan L'Her
erwan.lher@chu-brest.fr

[1] Médecine Intensive Et Réanimation, CHRU de La Cavale Blanche, Bvd. Tanguy-Prigent, 29609 BREST Cedex, France

[2] LATIM INSERM UMR 1101, Université de Bretagne Occidentale, BREST, France

1 Introduction

A major concern in mechanically ventilated patients is the risk of Ventilator-Induced Lung Injury (VILI). It has been demonstrated that protective ventilation using lower tidal volumes may reduce VILI, and improve prognosis [1]. Experimental studies demonstrated that spontaneous ventilation superimposed on mechanical ventilation may worsen lung injury while generating high transpulmonary pressure [2, 3]. These spontaneous breathing efforts may induce overstretch of dependent lung, associated with reciprocal deflation of nondependent lung, even when not modifying tidal volume [3]. The pattern of lung inflation may also be different in the presence of lung injury. The availability of a noninvasive global tidal volume monitoring technique, and the possibility to evaluate volume distribution may be of interest.

Recent data suggest that spontaneously breathing, nonintubated patients with acute respiratory failure may have a high respiratory drive, and may therefore breathe with large tidal volumes, thus potentially inducing Patient Self-inflicted Lung Injury (P-SILI) [4, 5]. Examples of patients without preexisting lung injury who develop lung injury associated with hyperventilation exist in the literature [6]. In the context of this high respiratory drive, lung-protective ventilation might be viewed not simply as supportive therapy in intubated patients, but as a prophylactic therapy to mitigate P-SILI in spontaneously breathing patients. However, such therapeutic concepts might require routine lung volume evaluation in nonintubated patients.

High-flow nasal cannula (HFNC) is increasingly used in the management of respiratory failure and it has proved to decrease the need for endotracheal intubation in patients with acute hypoxemic respiratory failure [7]. Via dedicated nasal cannula, the patient is administered a humidified gas flow at high levels (in between 30 to 60 L/min), at a variable inspiratory oxygen fraction (in between 21 and 100%). While HFNC seems to generate a low level of positive airway pressure and washout of dead space [8], little is known about its impact on tidal volume generation. If one may consider that volumes might be increased under HFNC while it generates a positive oropharyngeal airway pressure, volume measurement is not currently available. The question whether patients under HFNC do develop P-SILI due to the increased tidal volumes and minute ventilation seems probable [5].

There is a paucity of noninvasive, noncontact respiratory monitors for spontaneously breathing patients. Several studies have promoted the use of electrical impedance tomography (EIT) to evaluate lung volume under HFNC [9–16]. EIT is a bedside monitoring technique of the respiratory system that measures impedance changes within the thorax, thus providing dynamic volume distribution [17]. Most evaluations using EIT demonstrated that lung volumes might increase with increased gas flow. Other approaches for lung volume estimation during spontaneous ventilation include temperature profile changes through nasal canula or oxygen mask [18], microwave techniques [19] and optical-based techniques such as thermal imaging [20], structured light plethysmography [21], and optoelectronic plethysmography [22]. All these methods are either cumbersome and/or expensive, and/or only provide raw estimation of volumes, thus they cannot yet be applied for continuous monitoring in the ICU clinical routine.

Time-of-Flight imaging (TOF) is a novel noninvasive, noncontact, radiation-free, and easy-to-use technique, that provides direct volume measurement, without the use of any additional sensors. The technique is derived from standard volume surfacing measurements, that have been widely investigated in various situations [23–25]. Dellen et al. [26] have investigated the accuracy of the volume measurements using a commercial depth-sensing device, and calculated a 5.2% volume measurement error for medium size solid objects, with respect to the ground truth, while the depth accuracy for the Kinect V2 camera has been found to be of 2 mm [27].

It also enables to estimate on the same time differential volume distribution (e.g. left/right hemithorax or abdomen/thorax), thus being interesting to detect the occurrence of pneumothorax and/or atelectasis.

The primary objective of the study was to evaluate the accuracy of TOF volume and respiratory rate measurements within the ICU environment. The secondary objective was to detect if the technique could be implemented to monitor spontaneously breathing patients under HFNC.

2 Methods

2.1 Study design and population

Data analysis was performed within the ReaSTOC data-warehousing project including all patients admitted to our adult medical ICU (ClinicalTrials.gov identifier NCT02893462). A previous publication has already described the design of the Reastoc study [28]. The protocol was approved by our local ethics committee and written informed consent was waived, according to French legislation. The only exclusion criteria was the patient and/or relatives refusal to participate.

Clinical metadata were recorded using standard monitoring devices, and the computerized medical file (Intellivue MP70 and ICCA Philips Healthcare, Amsterdam, Netherlands). The first phase included all consecutive patients undergoing invasive mechanical ventilation (MV) included

within our database, thus enabling to collect the reference expired tidal volume (R860, GE Healthcare, Madison, WI, USA). Precision of the ventilator flow sensor was considered adequate while considering our purpose (± 10% or 10 mL with the ventilator's leak compensation activated) and the fact that it did not require any additional inline sensors that would have modified the setting and ethical approval of the ReaStoc project. The second phase included all consecutive patients undergoing HFNC that were analyzed using TOF.

All measurements were performed with the patient lying supine, with a 30° angulation of the bed head.

2.2 Volume acquisition

2.2.1 Device

TOF acquires the distance information based on measuring the phase delay between the emitted light-wave and back-scattered signals received by each photodetector. These cameras are capable of acquiring the distance from a few centimeters to several meters, and therefore are advantageously adapted for use in a clinical environment.

We used a Kinect V2 (Microsoft, Redmond, WA, USA), composed of a red, green, and blue (RGB) camera and an infrared (IR) emitter/detector that forms the depth sensor. The camera operational range is between 0.5 and 3.5 m; in the current study the system was placed on top of the patient's bed, at a distance of approximately 1.2 m from the patient (Fig. 1).

The measurement of respiratory parameters (tidal volume and respiratory rate) was performed by analyzing the changes of the chest wall position in the depth images, the movements of the chest wall being illustrated by the movements of external surfaces along the anteroposterior direction.

2.2.2 Autocalibration

TOF VT monitoring does not require calibration using a spirometer; the technique only requires an accurate orientation between the camera and the object of interest (patient), in order to optimize the depth measurement accuracy. As the movements of the lungs are illustrated by the movement of external surfaces along the anteroposterior direction, the camera plane is to be aligned perpendicularly to this direction. Therefore, calibration is performed automatically, based on a real time registration algorithm allowing a rigid transformation between the camera plane and the patient's thorax plane (see supplementary appendix for additional details).

2.2.3 Regions of interest (ROI) automated selection

The ROI are automatically selected, based on a deep neural network algorithm [29] that estimates human joints position. The algorithm predicts the location of various human "key points" such as elbows, knees, neck, shoulder, hips, chest(18 points including face and body features) [30]. Hence, the lower costal margin is detected, and the patient's torso is then defined by the surface connecting the joints of shoulders and hipbones. Monitoring of multiple ROI on the torso and right/left hemithorax separately enables detecting the presence of respiratory and volume distribution abnormalities (e.g. pneumothorax, atelectasis, diaphragmatic paradox) [31–33].

2.2.4 Tidal volume (VT) calculation

To smooth data, an exponential moving average filter was used to reduce random noise. Respiratory parameters are calculated based on the monitored respiratory signal. This

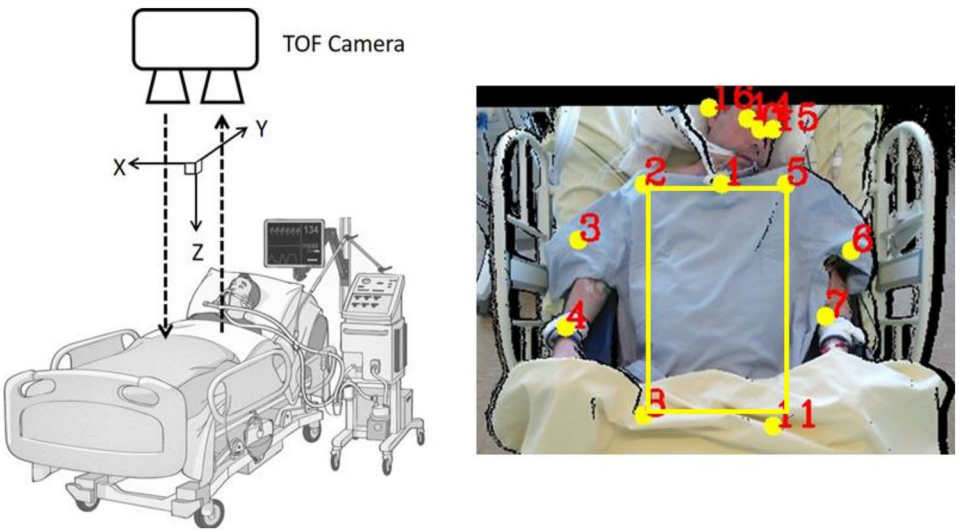

Fig. 1 Position of the TOF Camera and automatic determination of the regions of interest. The TOF camera is positioned perpendicularly at ~ 1.2 m from the patient's torso – it can be either fixed on the ceiling or on a moving trolley –the patient lying supine with a 30° angulation of the bed's head. Calibration is automated, as the ROI determination (yellow square). All red numbers corresponds to automated determination of the patient's points of interest and main joints. In case of discordance, position of the points of interest can be modified by the clinician

signal is obtained by analyzing the morphological changes in the chest wall. The 1D signal is obtained by calculating the differences between the spatial average of the depth values in the image at a given time and the spatial average of the depth values of a reference image in given ROI defined on the torso of the patient. The volume-time curve computed by estimating the volume of the ROI as a function of time is obtained as:

$$V(k) = D(k) \times S \times 10^3$$

wherein D(k) is the measure of average depth variation estimated for *k,* the image of the acquisition sample, and S is a parameter representing the surface of the ROI quantified in mm^2, and the multiplicative factor 10^3 is the conversion from a volume in mm^3 to a volume quantified in mL.

The volume time curve presents a peak for each inhalation and a valley for each exhalation of the patient. Therefore, the tidal volume which is the volume of air passing in or out the lungs in a cycle, is calculated by subtracting the lung volume of the corresponding extrema points. To improve accuracy and eliminate aberrant values, the recorded tidal volume value is considered as the average of all detected inspiratory peak, over a one minute recording window. The calculations were automatically and continuously performed on clinical data over a stable period of at least 10 to 20 min. acquisition per patient (*i.e.* 10 to 20 recorded values per patient).

2.3 Respiratory rate calculation

The respiratory rate (RR) is considered to be the number of breathing cycles in one ventilation minute. It is calculated by counting the number of peaks in V(k) in a time interval of one minute. The relevant peaks in the signal are detected based on the calculation of the maxima and minima within a window. The maxima should be greater than a threshold defined as the average of the first seconds of the respiratory signal (Fig. 2).

2.4 Reference VT and RR

2.4.1 Reference values were those recorded within the ReaStoc database

Reference VT was recorded as the mean expiratory value provided by the ventilator each minute, over a stable period of 10 to 20 min. Such period was chosen to improve accuracy and eliminate aberrant values while instant VT values are not always accurate (several artefacts due to external factors, such as humidification, active patient's expiration, movements …).

RR was considered as the mean value measured by either the ventilator or a manual chronometric evaluation, over a 60 s. period for patients under HFNC. A 60 s. period was chosen as a reference, while for manual chronometric evaluation shorter intervals, equal or below 15 s., are considered less accurate [28].

2.5 Statistical analysis

Continuous variables were expressed as mean ± SD; categorical variables were expressed as numbers and percentages. Data normality was assessed using the D'Agostino-Pearson normality test.

Under mechanical ventilation, ventilator respiratory rate and expired VT were regarded as the reference methods and TOF measurements as the method of comparison. Under HFNC, no comparative value was available for VT and manual chronometric evaluation over 30-s. period was considered as the reference for RR.

Linear correlation between the different methods was performed using Pearson's correlation coefficient analysis. The agreement between quantitative measure of the reference and the estimated VT and RR values was graphically appreciated according to Bland and Altman [34].

Statistical significance was defined as a two-tailed *P*-value of < 0.05 for all analyses. Analyses were performed using MedCalc Statistical Software version 18.6 (MedCalc Software bvba, Ostend, Belgium).

3 Results

Fourty four patients were recorded, of which 32 patients were under invasive mechanical ventilation (MV), and 12 others were spontaneously breathing under HFNC. Physiological characteristics for patients under MV are depicted within Table 1. First cause of admission was respiratory failure, and almost 40% of the patients under mechanical ventilation were presenting patient-ventilator asynchronies.

Four hundred eighty six and 505 measurements were performed under MV, for VT and RR respectively. The degrees of agreement between the estimated and reference values (VT and RR) are reported within Fig. 3. The scatter plot and linear regression for VT depicted high correlation ($r = 0.84$; $p < 0.001$), with a low bias (-1.7 mL) and acceptable deviation (~ 75 mL); the percentage of error for VT was equal to $-0.5 \pm 8.1\%$. The scatter plot and linear regression for RR depicted high correlation ($r = 0.91$; $p < 0.001$), with a low bias (< 1 b/min) and acceptable deviation (≤ 5 b/min)); the percentage of error for RR was equal to $3.1 \pm 11.0\%$.

Measurements were possible in all 12 spontaneously breathing patients under HFNC (Table 2). RR_{TOF} evaluation was similar to the reference value that was measured manually, with a good correlation (26 ± 5 vs. 27 ± 4 b/min for Reference and TOF respectively; $r = 0.86$; $P < 0.001$).

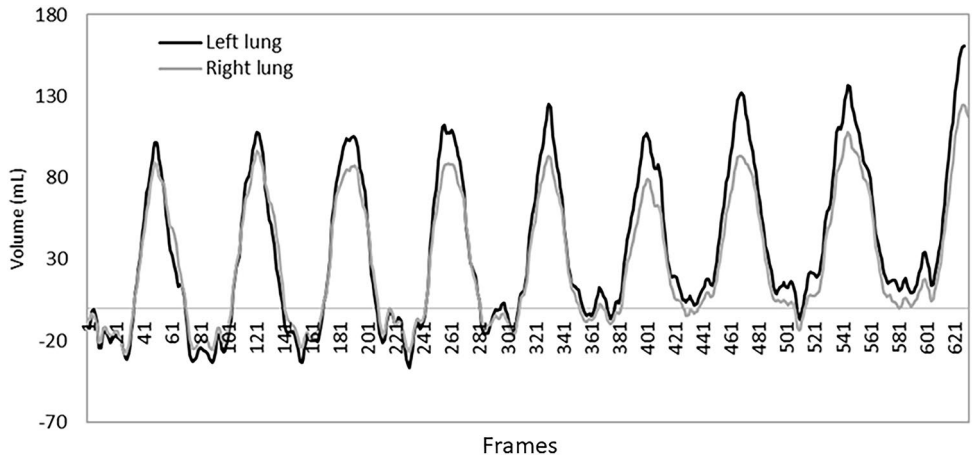

Fig. 2 Monitoring of the left and right hemithoraces. Regional ventilation monitoring of the left and right patient's hemithoraces is depicted. The volume time curve is obtained by analyzing the right and left hemithoraces ROIs separately. The black curve corresponds to the volume time curve of the right thorax and the gray curve corresponds to the volume time curve of the left thorax. Such analysis may enable to depict regional abnormalities such as atelectasis and/or pneumothorax

While mean VT under HFNC was within the 6–8 mL/kg target range, 4/12 patients were developing VT > 8 mL/kg and 6/12 VT < 6 mL/kg (Table 3). For these patients outside VT range, flow was maximal in all cases (60 L/min); in one case (VT > 8 mL/kg), decreasing flow resulted in a decreased VT and no RR modification; in two cases (VT < 6 mL/kg), decreasing flow resulted in an increased VT and decreased RR; in one case (VT < 6 ML/kg), decreasing flow resulted in a decreased VT and increased RR.

4 Discussion

In ICU patients requiring mechanical ventilation, TOF proved to be correlated to the expiratory VT measured by the ventilator. VT values that were obtained with TOF under HFNC enabled the evaluation of the impact of flow modifications, and depicted at least one patient with significant overdistension related to high-flow administration.

EIT is a bedside noninvasive monitoring technique that measures the voltage response of biological tissues to an externally applied alternating electric current [35] and therefore provides indirect evaluation of global volume distribution, and an estimate of regional VT in the studied chest slice [17, 35]. Its clinical applications are to quantify lung collapse, tidal recruitment and lung overdistension under mechanical ventilation. It has also been proposed to evaluate the effects of flow variation on lung recruitment and overdistension under HFNC [36, 37]. Ventilation assessment is a correlation of global impedance, unless tidal volume is measured by an external reference (*e.g.*, spirometry), EIT tidal volume cannot be determined. While such scaling and calibration is easily feasible under mechanical ventilation, it may become more difficult for spontaneously breathing patients. The technique requires direct contact with the patient, since it uses a belt placed at the patient's chest, and applies an alternating current through the implemented electrodes (from 8 to 32, according to the commercial device). The location of the electrode plane may impact the findings. The alternating electric currents used during EIT are safe for a body application, undetected by the patients, but its use in patients with pacemakers and defibrillators is not recommended.

Several non-invasive and non-contact sensing techniques of human beings have been conceived, mainly within the security and safety domains, but only a very few have reached the clinical setting. The Linshom temperature profile tracks changes in VT in healthy volunteers [18]. In such experimental conditions, it was considered as a simple and reliable technique to estimate tidal volume under spontaneous ventilation. However, it was never tested with HFNC, and further studies are warranted in clinical settings to establish its effectiveness in the ICU setting. Different techniques using microwave sensors have been promoted to detect vital signs, either with continuous wave (CW) or ultra-wideband radars [38, 39]. While most of these techniques seemed interesting for heart rate and RR monitoring without contact, they have been rarely evaluated for lung volume assessment. One team evaluated its capability to quantify lung volumes [19]; accuracy of the VT estimation was not very high, and the new technique needed a preliminary calibration with a spirometer for every subject. Optical-based monitoring techniques might offer several perspectives within the ICU. Thermal imaging mainly enables RR monitoring [20, 40].

Table 1 Physiological characteristics of the patients

General characteristics *(n = 44)*	
Age *(years)*	63 ± 14
Sex ratio *(Female/Male)*	10/34
BMI *(kg/m²)*	27.2 ± 8.0
SAPS 2	52.6 ± 17.7
SpO_2/FIO_2	321 ± 123
Admission diagnosis	
Respiratory failure *n-(%)*	22 (50.0%)
Cardiovascular failure *n-(%)*	8 (18.2%)
Neurological failure *n-(%)*	14 (31.8%)
Mechanical ventilation characteristics *(n = 32)*	
Invasive MV *n-(%)*	32 (72.7%)
Intravenous sedation *n-(%)*	18 (40.9%)
Paralyzing agents *n-(%)*	1 (2.3%)
PEEP *(cm H_2O)*	6.0 ± 1.9
Ventilatory mode *n-(%)*	29 (65.9%) ACV / 3 (6.8%) PSV
Patient/Ventilator Asynchrony *n-(%)*	13 (29.5%)

Results are depicted as mean ± STD and n(%). Most patients were admitted for an acute respiratory failure and required invasive mechanical ventilation. Within the ReaSTOC datawarehouse, Patient/Ventilator Asynchrony are assessed for 10-min. at the bedside according to ventilator curves evaluation; a manually calculated asynchrony index higher than 10% was considered significant

Structured light plethysmography (SLP) is a very interesting technique that offers non-contact, self-calibrating evaluation of lung volumes. A commercial device already exists (PneumaCare Thora-3DI™) and significant benefits may occur for clinical assessment of chest wall motion abnormalities [21]. However structured light cameras devices are rather expensive (> 25 000 € for the commercially available device), and the technique has mainly been used in a pediatric population [41], and never within the adult ICU environment. Optoelectronic plethysmography (OEP) is another optic method to measure chest wall movements and estimate accurately lung volumes [22]. However, while it is based on the general principles of 3D motion capture, it requires the placement of numerous chest sensors and the use of multiple cameras, thus making it impossible to be used in the clinical setting.

Unlike other available non-contact and/or optic methods, TOF is advantageously able to calculate either global and regional pulmonary function, using a single low cost depth camera and no additional sensors. It enables assessment of the respiratory volume of either left/right hemithorax, and abdominal regions separately. The accuracy of the deep learning neural network that was used for ROI detection has been proved to reach a 88.8% value [42]. Afterwards, the local analysis is performed by defining the corresponding region of interest and applying the same methodology described above to extract respiratory signals of each region and calculate the respiratory parameters. The abdominal region includes the surface between the diaphragm and the hip bones, the left hemithorax region may be defined on the left side of the rib cage so as to cover the left lung, and a right hemithorax region may be defined on the right side of the rib cage so as to cover the right lung. Variation of the thorax size and lung volumes due to the inspiration and expiration are illustrated by the movement of chest wall's external surfaces along the anteroposterior direction. The benefits of the technique are the autocalibration method that was implemented within the algorithm, the accuracy of measurements, and the relatively low cost of the technique. Considering such potential benefits, TOF could be used to evaluate lung overdistension under HFNC, and to help clinicians' care, while simple TOF measurements prior and after each flow changes may enable to verify that the patient generates a VT value within the adequate range. It may particularly help detecting patients at risk of P-SILI, while generating high VT. Similar use could be proposed for patients with acute respiratory failure under noninvasive ventilation and CPAP. Continuous TOF measurements could also help to evaluate PEEP changes in ARDS patients, based on the single-breath recruitability assessment maneuver [43], but also be valuable for atelectasis, pleural effusions and/or pneumothorax detection while considering left/right hemithoraces expansion symmetry. Such hypothesis may however require further investigations for validation. Even if all measurements in the current study were performed with the patient lying supine with a 30° bed head angulation,due to the spatial calibration of the algorithm, our technology has the advantage of monitoring the patients in various positions (Supine, Fowler's, Semi-Fowler's, in a bed or in a chair), while the important thing is to maintain perpendicularity between the camera and the torso. The accuracy of TOF monitoring may be affected by the items covering the patient (*e.g.* cover, blanket, gown) if the thoracic motion is too small to be detected by the camera. The patient population that was included in the current study included skin exposed patients, patients wearing gowns or covered by a blanket, as in clinical routine. While the ROI detection algorithm may fail with patients covered by a blanket, we did not notice any particular effects of patient clothing on depth measurement accuracy.

TOF monitoring may also be proposed for continuous VT monitoring of unstable spontaneously breathing patients to detect alveolar hypoventilation such as in the operation recovery room. The technique may therefore cover new areas of monitoring under respiratory assistance. Still more work is needed to develop and interpret TOF measurements, and its possible combination with EIT indices to guide the clinician towards effective and safe respiratory assistance.

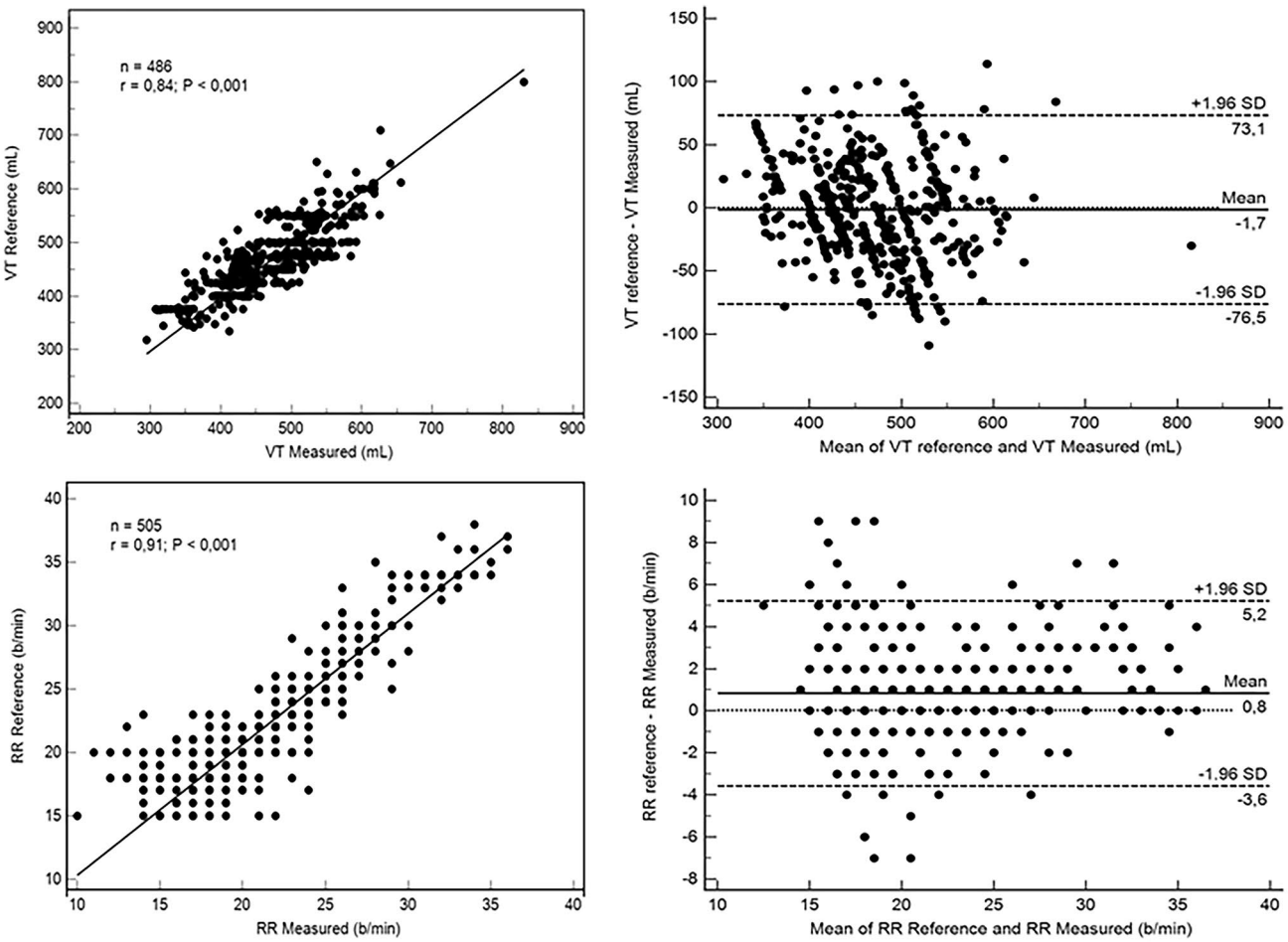

Fig. 3 Correlation and Bland–Altman plot for reference and estimated respiratory rate and tidal volume. All measurements were performed with the patient lying supine, with a 30° angulation of the bed head. Values are provided as breath per minute (bpm) for the reference respiratory rate (RR) and mL for the tidal volume (Vt). RR values were provided by its chronometric measurement at the bedside during a 60-s period. Reference Vt values were provided by the ventilator expiratory flowmeter for patients under ventilatory assistance. Estimated RR and Vt were performed using the TOF based monitoring system over a 60-s period. On the 31 ICU patients' recordings, the estimation of the RR and Vt was well correlated with the reference method (Fig. 2-A; $R = 0.9$; $p < 0.0001$ / Fig. 2-C; $R = 0.8$; $p < 0.0001$). Comparison of the methods using the Bland–Altman method depicted a very low bias for RR (Fig. 2-B; 1 bpm) and Vt (Fig. 2-D; -1 mL) and an acceptable deviation ($< \pm 3.7$ bpm and 80 mL, respectively)

Several limitations of our study must be highlighted. First, one may consider that too few patients were included to firmly validate the accuracy of our results, and that the reference VT value (expiratory VT measurement extracted from the ventilator) may be questionable. However, the overall number of VT and RR measurements over time (> 480 measurements), combined with the excellent correlation of both values with a low bias enables TOF to be considered as a valuable tool. Moreover, most important references depicting benefits from tidal volume monitoring, especially in ARDS patients, used such measurements as a therapeutic goal [44]. The overall precision of the ventilator expiratory sensor (± 10% or 10 mL) seems accurate from a clinical perspective. Second, while this was an observational physiological study, the low number of flow variations under HFNC cannot provide sufficient data to validate the use of TOF to monitor such patients in routine and help adjust settings. Third, several limitations and/or potential biases related to the use of the ReaStoc database for VT and RR reference values should also be discussed. No raw breath-by-breath analysis was performed for VT and RR, according to the design of the database. We did consider that modifying the way to measure reference values would have a-modified the ethical approval for the database, b- introduced biases related to artefacted values.

Table 2 Patients characteristics under HFNC

Number of Patients	12
Sex ratio *(Female/Male)*	1/11
Age *(year)*	55.9 ± 19.7
SAPS 2	37.7 ± 16.1
SpO_2/FIO_2	170 ± 55
Baseline Flow *(L/min)*	55 ± 7
FIO_2 *(%)*	59 ± 20
RR_{Ref} *(b/min)*	27 ± 4
RR_{TOF} *(b/min)*	26 ± 5
VT_{TOF} *(mL)*	429 ± 125
VT_{TOF} *(mL/kg IBW)*	6.5 ± 2.1

Results are depicted as mean ± STD. RR_{Ref}: manually calculated respiratory rate reference. RR_{TOF}: respiratory rate calculation provided by the TOF device. VT_{TOF}: tidal volume calculated by the TOF device. Most patients were receiving high flow rates

Table 3 Individual baseline data acquisition for patients under HFNC

Patients (n°)	VT_{TOF} (mL)	VT_{TOF} (mL/kg IBW)	Flow (L/min)
1	492	7,9	40
2	469	6,0	60
3	308	**4,2**	50
4	640	**9,8**	60
5	534	**8,2**	60
6	285	**5,3**	60
7	384	**5,9**	50
8	286	**3,7**	60
9	487	**8,7**	60
10	599	**8,9**	50
11	355	**5,2**	50
12	309	**4,6**	60

VT considered outside range (6–8 mL/kg) are depicted in bold character; in grey box for VT below range, in pale blue for VT higher than the range. Patient 4 had to be intubated due to severe hypoxic respiratory failure

In conclusion, VT_{TOF} is correlated to VT_{Ref}. TOF enables continuous and non-contact VT monitoring under HFNC, and is able to detect VT and RR changes while modifying flow.

Acknowledgements None

Authors' contribution ELH is the primary investigator of the ReaSTOC study, acquired and analyzed data, drafted the manuscript. SN and VP acquired, analyzed data and drafted the manuscript. DV drafted the manuscript. All authors finally approved the manuscript.

Funding The study was funded by the programme de maturation SDSP-DV2896/LATIM**;** Ouest Valorisation.

Data availability All data will be available upon reasonable request.

Declarations

Conflict of interest ELH, SN, DV are co-inventors of the technique (Body surface optical imaging for respiratory monitoring; European patent application No. 19306417.7–1115. ELH is a co-founder and shareholder of Oxynov Inc., a Canadian R&D company; he is also consultant for GE Healthcare, Smiths, Sedana Medical. VP, SN, DV have no other conflicts of interest.

Ethical approval Data analysis was performed within the ReaSTOC data-warehousing project including all patients admitted to our adult medical ICU (ClinicalTrials.gov identifier NCT02893462). The protocol was approved by our local ethics committee and written informed consent was waived, according to French legislation.

Consent for publication Not applicable.

References

1. The Acute Respiratory Distress Syndrome Network. Ventilation with Lower Tidal Volumes as Compared with Traditional Tidal Volumes for Acute Lung Injury and the Acute Respiratory Distress Syndrome. N Engl J Med. 2000;342:1301–8.
2. Yoshida T, Uchiyama A, Matsuura N, Mashimo T, Fujino Y. Spontaneous breathing during lung-protective ventilation in an experimental acute lung injury model: high transpulmonary pressure associated with strong spontaneous breathing effort may worsen lung injury. Crit Care Med. 2012;40:1578–85.
3. Yoshida T, Torsani V, Gomes S, et al. Spontaneous effort causes occult pendelluft during mechanical ventilation. Am J Respir Crit Care Med. 2013;188:1420–7.
4. Grieco DL, Menga LS, Eleuteri D, Antonelli M. Patient self-inflicted lung injury: implications for acute hypoxemic respiratory failure and ARDS patients on non-invasive support. Minerva Anestesiol. 2019;85:1014–23.
5. Brochard L, Slutsky A, Pesenti A. Mechanical ventilation to minimize progression of lung injury in acute respiratory failure. Am J Respir Crit Care Med. 2017;195:438–42.
6. Brun-Buisson CJ, Bonnet F, Bergeret S, Lemaire F, Rapin M. Recurrent high-permeability pulmonary edema associated with diabetic ketoacidosis. Crit Care Med. 1985;13:55–6.
7. Rochwerg B, Granton D, Wang DX, et al. High flow nasal cannula compared with conventional oxygen therapy for acute hypoxemic respiratory failure: a systematic review and meta-analysis. Intensive Care Med. 2019;45:563–72.
8. Mündel T, Feng S, Tatkov S, Schneider H. Mechanisms of nasal high flow on ventilation during wakefulness and sleep. J Appl Physiol. 2013;114:1058–65.
9. Corley A, Caruana LR, Barnett AG, Tronstad O, Fraser JF. Oxygen delivery through high-flow nasal cannulae increase end-expiratory lung volume and reduce respiratory rate in post-cardiac surgical patients. Br J Anaesth. 2011;107:998–1004.
10. Fraser JF, Spooner AJ, Dunster KR, Anstey CM, Corley A. Nasal high flow oxygen therapy in patients with COPD reduces respiratory rate and tissue carbon dioxide while increasing tidal and end-expiratory lung volumes: a randomised crossover trial. Thorax. 2016;71:759–61.
11. Mauri T, Alban L, Turrini C, et al. Optimum support by high-flow nasal cannula in acute hypoxemic respiratory failure: effects of increasing flow rates. Intensive Care Med. 2017;43:1453–63.

12. Okuda M, Tanaka N, Naito K, et al. Evaluation by various methods of the physiological mechanism of a high-flow nasal cannula (HFNC) in healthy volunteers. BMJ Open Respir Res. 2017;4:e000200.
13. Parke RL, Bloch A, McGuinness SP. Effect of very-high-flow nasal therapy on airway pressure and end-expiratory lung impedance in healthy volunteers. Respir Care. 2015;60:1397–403.
14. Plotnikow GA, Thille AW, Vasquez DN, et al. Effects of high-flow nasal cannula on end-expiratory lung impedance in semi-seated healthy subjects. Respir Care. 2018;63:1016–23.
15. Riera J, Pérez P, Cortés J, Roca O, Masclans JR, Rello J. Effect of high-flow nasal cannula and body position on end-expiratory lung volume: A cohort study using electrical impedance tomography. Respir Care. 2013;58:589–96.
16. Yuan Z, Han X, Wang L, et al. Oxygen therapy delivery and body position effects measured with electrical impedance tomography. Respir Care. 2019;65:281–7.
17. Frerichs I, Amato MB, van Kaam AH, et al. Chest electrical impedance tomography examination, data analysis, terminology, clinical use and recommendations: consensus statement of the TRanslational EIT developmeNt stuDy group. Thorax. 2017;72:83–93.
18. Sathyamoorthy M, Lerman J, Amolenda PG, Wilson GA, Feldman R, Moser J, Feldman U, Abraham GE 3rd, Feldman D. Tracking tidal volume noninvasively in volunteers using a tightly controlled temperature-based device: A proof of concept paper. Clin Respir J. 2020;14:260–6.
19. Dei D, Grazzini G, Luzi G, Pieraccini M, Atzeni C, Boncinelli S, Camiciottoli G, Castellani W, Marsili M, Dico JL. Non-contact detection of breathing using a microwave sensor. Sensors. 2009;9:2574–85.
20. - Chekmenev Y, Rara H, Farag A. Non-contact, wavelet-based measurement of vital signs using thermal imaging. in Proc. ICGST Int.Conf.Graph,Vision and Image Processing,Cairo,Egypt,Dec. 2005, pp. 25–30.
21. Fleck D, Curry C, Donnan K, Logue O, Graham K, Jackson K, Keown K, Winder J, Shields MD. Hughes CM (2019) Investigating the clinical use of structured light plethysmography to assess lung function in children with neuromuscular disorders. PLoS ONE. 2019;14:e0221207.
22. Romagnoli I, Lanini B, Binazzi B, Bianchi R, Coli C, Stendardi L, Gigliotti F, Scano G. Optoelectronic Plethysmography has Improved our Knowledge of Respiratory Physiology and Pathophysiology. Sensors. 2008;8:7951–72.
23. - Fankhauser P, Bloesch M, Rodriguez D, Kaestner R, Hutter M, Siegwart R. Kinect v2 for mobile robot navigation: Evaluation and modeling. In: *2015 International Conference on Advanced Robotics (ICAR)*. IEEE; 2015:388–394.
24. - Wasenmüller O, Stricker D. Comparison of Kinect v1 and v2 depth images in terms of accuracy and precision. In: *Asian Conference on Computer Vision*. Springer; 2016:34–45.
25. - Ollikkala AVH, Mäkynen AJ (2007) Use of time-of-flight 3D camera in volume measurements. Proc. SPIE 7022, Advanced Laser Technologies, 702219 (5 June 2008).
26. - Dellen, B., & Rojas Jofre, I. A. (2013). Volume measurement with a consumer depth camera based on structured infrared light. In *Proceedings of the 16th Catalan Conference on Artificial Intelligence, poster session* (pp. 1–10).
27. Yang L, Zhang L, Dong H, Alelaiwi A, El Saddik A. Evaluating and improving the depth accuracy of Kinect for Windows v2. IEEE Sens J. 2015;15:4275–85.
28. L'Her E, N'Guyen QT, Pateau V, Bodenes L, Lellouche F. Photoplethysmographic determination of the respiratory rate in acutely ill patients: validation of a new algorithm and implementation into a biomedical device. Ann Intensive Care. 2019;9:11.
29. Sun Y, Xue B, Zhang M, Yen GG. Evolving deep convolutional neural networks for image classification. IEEE Trans Evol Comput. 2019;24:394–407.
30. Nazir S, Pateau V, Bert J, Clement JF, Fayad H, L'Her E, Visvikis D. Surface imaging for real-time patient respiratory function assessment in intensive care. Med Phys. 2021;48:142–55.
31. Liu H, Guo S, Liu H, et al. The best body spot to detect the vital capacity from the respiratory movement data obtained by the wearable strain sensor. J Phys Ther Sci. 2018;30:586–9.
32. Johnston CR 3rd, Krishnaswamy N, Krishnaswamy G. The Hoover's Sign of Pulmonary Disease: Molecular Basis and Clinical Relevance. Clin Mol Allergy. 2008;6:8.
33. Garcia-Pachon E. Paradoxical movement of the lateral rib margin (Hoover sign) for detecting obstructive airway disease. Chest. 2002;122:651–5.
34. Bland JM, Altman DG. Statistical method for assessing agreement between two methods of clinical measurement. The Lancet. 1986;1:307–10.
35. Putensen C, Hentze B, Muenster S, Muders T. Electrical impedance tomography for cardio-pulmonary monitoring. J Clin Med. 2019;8:1176.
36. Zhang R, He H, Yun L, et al. Effect of postextubation high-flow nasal cannula therapy on lung recruitment and overdistension in high-risk patient. Crit Care. 2020;24:82.
37. Yuan Z, Han X, Wang L, et al. Oxygen therapy delivery and body position effects measured with electrical impedance tomography. Respir Care. 2020;65:281–7.
38. Droitcour AD, Boric-Lubecke O, Lubecke VM, Lin J, Kovacs GTA. Range correlation and I/Q performance benefits in single-chip silicon Doppler radars for noncontact cardiopulmonary monitoring. IEEE Trans Microw Theory Tech. 2004;52:838–48.
39. Xiao Y, Li C, Lin J. A portable noncontact heartbeat and respiration monitoring system using 5-GHz radar. IEEE Sens J. 2007;7:1042–3.
40. Procházka A, Charvátová H, Vyšata O, Kopal J, Chambers J. Breathing analysis using thermal and depth imaging camera video records. Sensors. 2017;17:1408.
41. Ghezzi M, Tenero L, Piazza M, Zaffanello M, Paiola G, Piacentini GL. Feasibility of structured light plethysmography for the evaluation of lung function in preschool children with asthma. Allergy Asthma Proc. 2018;39:e38–42.
42. Cao Z, Hidalgo G, Simon T, Wei SE, Sheikh Y. OpenPose: real-time multi-person 2D pose estimation using Part Affinity Fields. IEEE Trans Pattern Anal Mach Intell. 2019;43:172–86.
43. Chen L, Del Sorbo L, Grieco DL, et al. Potential for lung recruitment estimated by the recruitment-to-inflation ratio in acute respiratory distress syndrome. A clinical trial. Am J Respir Crit Care Med. 2020;201:178–87.
44. Network ARDS, Brower RG, Matthay MA, Morris A, Schoenfeld D, Thompson BT, Wheeler A. Ventilation with lower tidal volumes as compared with traditional tidal volumes for acute lung injury and the acute respiratory distress syndrome. N Engl J Med. 2000;342:1301–8.